Chinese Chemical Letters 35 (2024) 108925

Contents lists available at ScienceDirect

Chinese Chemical Letters

journal homepage: www.elsevier.com/locate/cclet

An AIEgen nano-assembly for simultaneous detection of ATP and H_2S

Jia-Mei Qin[1], Xue Li[1], Wei Lang[1], Fu-Hao Zhang, Qian-Yong Cao*

School of Chemistry and Chemical Engineering, Nanchang University, Nanchang 330031, China

ARTICLE INFO

Article history:
Received 20 June 2023
Revised 8 August 2023
Accepted 9 August 2023
Available online 12 August 2023

Keywords:
AIE-based
ATP detection
H_2S detection
Fluorescent sensor
Cell imaging

ABSTRACT

A new aggregation-induced emission (AIE)-based fluorescence sensor, **TPEPy-SS-C14**, for simultaneous recognition of adenosine triphosphate (ATP) and hydrogen sulfide (H_2S) has been reported *via* the aggregation-disaggregation mechanism. The probe self-assembles nano-structure aggregations in aqueous solution. It shows fluorescence turn-on response toward ATP for the complexation-enhanced aggregation, but leads to fluorescence quenching of H_2S for cleavage the aggregations.

Adenosine triphosphate (ATP), known as "the energy currency of the cell", plays an important role in living cells, including protein synthesis, intracellular signal transduction and cell division [1,2]. The abnormal levels of intracellular ATP have been proved to be closely associated with a variety of diseases, such as cancer and Parkinson [3]. On the other hand, as a signal molecule, hydrogen sulfide (H_2S) widely exists in heart, brain, liver and other major organs, and plays an irreplaceable role in physiological functions including neural regulation, apoptosis, insulin signal inhibition and blood pressure [4]. The normal concentration of H_2S in cells is about 0.01–3 μmol/L [5]. Abnormal H_2S level can lead to the disfunction of cell, which is related to many diseases, like cirrhosis and Alzheimer's disease [6]. Therefore, the detection of ATP and H_2S level has important physiological and pathological significance.

Recently, fluorescent sensors of ATP and H_2S within cellular environments are well developed for the fast response, excellent selectivity, high sensitivity and simple operation of the fluorescent technique [7]. The ATP sensors are mainly on the basis of the different host-guest interaction mechanism, for instance, metal ion complexation, hydrogen bonding, π-π interaction and the electrostatic interaction [8–12], while the recognition of H_2S is based on the different types of chemical reaction, including copper sulfide precipitation, nucleophilic addition and reductive reaction [13,14]. Nevertheless, the traditional sensors are mainly limited to detect single species, fluorescent sensors for the simultaneous recognition of ATP and H_2S are still rare.

Currently, fluorescent sensors for simultaneous detection dual or multiple chemical species in biology have attracted much attention [15–17]. Some multifunctional fluorescent sensors for ATP and another analyte, including H_2O_2, H_2S, $ONOO^-$ and nitroreductase (NTR), were also documented [18–23]. Typically, the multi-analyte chemosensors were elegantly prepared by covalently linked multiple analyte recognition sites, including complexation and chemical reaction, with one or two flurophores in a single molecule. This strategy requires cumbersome chemical synthesis methods and is time-consuming and labor-intensive.

Aggregation-induced emission (AIE) fluorogens, also named as AIEgens, which have attracted much attention for their unique fluorescence emission properties [24]. The AIEgens show non- or weak emission in dilution solutions, but emit strongly at the aggregation state. Previously, we have reported imidazolium-functionalized tetraphenylethylenes, which have a good fluorescence turn-on sensing toward ATP for the complexation enhanced aggregation [25]. We envisioned that if the second recognition site such as the disulfide bond is rationally incorporated into this system, a dual functional probe which can detect ATP and another analyte will be obtained. In this context, herein, we design and synthesize a novel AIE bifunctional probe **TPEPy-SS-C14** (Scheme 1), which can simultaneously detect ATP and H_2S based on the aggregation/disaggregation mechanism. The probe **TPEPy-SS-C14** is rationally designed as following: (1) The TPEPy unit makes probe a red AIE-based emission, (2) the pyridinium and amide groups are used as the ATP binding site *via* the electrostatic interactions and hydrogen bonding, (3) the disulfide bond is cleavable by H_2S, and

* Corresponding author.
E-mail address: cqyong@ncu.edu.cn (Q.-Y. Cao).
[1] These authors contributed equally to this work.

https://doi.org/10.1016/j.cclet.2023.108925
1001-8417/

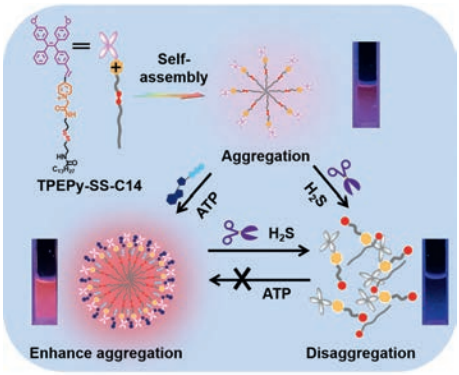

Scheme 1. Chemical structure of **TPEPy-SS-C14** and its proposed response mechanism to ATP and H_2S.

(4) the long alkyl chain endows probe a good amphiphilic property in aqueous solution. In addition, the probe locates mitochondria, and can detect ATP and hydrogen sulfide levels in living cells.

The detailed synthesis route of **TPEPy-SS-C14** is shown in Scheme S1 (Supporting information). And the chemical structure of **TPEPy-SS-C14** was verified by high-resolution mass spectrometry (HRMS), ^1H nuclear magnetic resonance (NMR) and ^{13}C NMR spectra (Figs. S1-S5 in Supporting information).

Firstly, the ultraviolet–visible (UV–vis) absorption and fluorescence spectra of **TPEPy-SS-C14** (10 μmol/L) was investigated in aqueous solution. As shown in Fig. 1a, **TPEPy-SS-C14** exhibits a red emission with the maximum peak at 630 nm and a low-energy absorption peak at 428 nm. The Stokes shift is 202 nm, which can prevent the interference effectively caused by self-absorption in the excitation process of biological imaging.

Next, the AIE properties of **TPEPy-SS-C14** were studied by emission spectra in water/DMSO mixture (Figs. 1b and c). In DMSO, the soluble **TPEPy-SS-C14** molecule shows very weak emission at 630 nm. The fluorescence intensity of **TPEPy-SS-C14** increased gradually with the increasing fraction of water and attained the maximum intensity in 90% aqueous solution, which may be due to the formation of nano aggregates. Additionally, the Tyndall experiment, scanning electron microscopy (SEM) and dynamic light scattering (DLS) measurements well confirmed the formation of nona-aggregation. The **TPEPy-SS-C14** aggregations show a sphere morphology with a diameter of 160–180 nm (Fig. 1d). Besides, the critical micelle concentration (CMC) of **TPEPy-SS-C14** was also investigated by concentration-dependent fluorescence experiment in aqueous solution, with the calculated value of 7.78 μmol/L, lower than the concentration used for testing (10 μmol/L, Fig. S6 in Supporting information).

We evaluated the sensing properties of **TPEPy-SS-C14** toward ATP in 4-(2-hydroxyethyl)–1-piperazineethanesulfonic acid (HEPES) aqueous buffer solution (pH 7.4). With the addition of ATP, the fluorescence of **TPEPy-SS-C14** gradually increased and got saturated when 17 equiv. ATP was added (Fig. 1e), with the fluorescence emission intensity at 630 nm about 3.6-fold enhancement. In addition, according to fluorescence titration data, the binding constant of **TPEPy-SS-C14** and ATP is calculated to be 2.57×10^5 mol/L and the stoichiometric binding ratio is 1:1 (Fig. S7a in Supporting information). The detection limit of **TPEPy-SS-C14** towards ATP is 12.3 nmol/L (Fig. S7b in Supporting information), indicating that the probe can recognize ATP quantitatively and effectively in physiological conditions.

Next, the fluorescence responding of **TPEPy-SS-C14** toward H_2S alone was also investigated. In Fig. 1f, upon the increasing concentration of sodium sulfide, the fluorescence of **TPEPy-SS-C14** will gradually decrease, with the quenching ratio about 80% when 55 equiv. sodium sulfide was added. This change can be well observed by the naked eye under the irradiation of a 365 nm ultraviolet lamp, along with the fluorescence color varying from red fluorescence to dark luminescence. The fluorescence intensity at 630 nm *versus* the concentration of hydrogen sulfide exhibits a great linear relation from 0 to 200 μmol/L, and the calculated limit of detection (LOD) is 5.0×10^{-7} mol/L (Fig. S8 in Supporting information). Then the time-dependent fluorescence spectra of **TPEPy-SS-C14** added with 40 equiv. H_2S were investigated. The fluorescence of probe decreases rapidly in a few seconds and basically reaches equilibrium in three minutes, which indicates that **TPEPy-SS-C14** can be used for rapid detection of H_2S (Fig. S9 in Supporting information).

Compared to other reported probes for simultaneous detection of ATP and H_2S (Table S1 in Supporting information), **TPEPy-SS-C14** has a lower detection limit and shorter detection time [18–23]. These listed probes are all using rhodamine linked 1,8-naphthalimide as fluorescence signal matrix, which can recognize ATP through the spirolactam ring-opening mechanism of

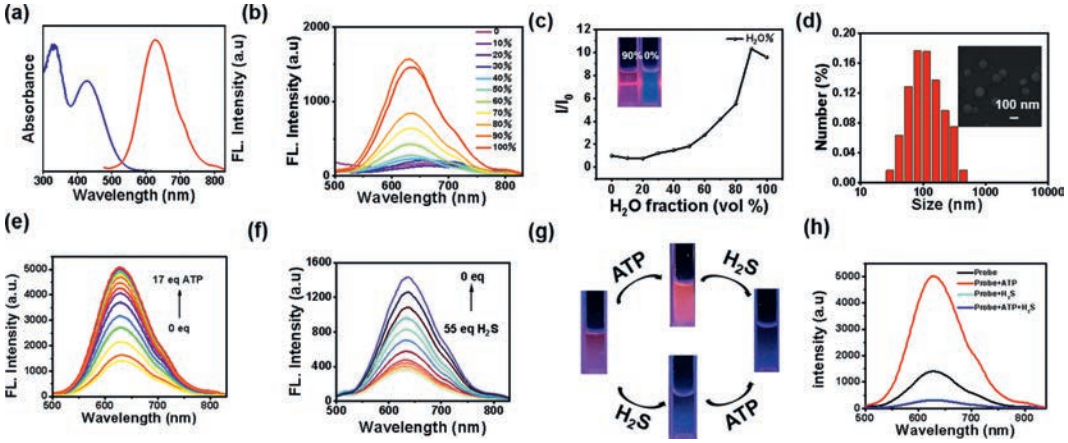

Fig. 1. (a) UV–vis absorption and emission spectra of **TPEPy-SS-C14** (10 μmol/L) in HEPES (10 mmol/L, pH 7.4) buffer solution. (b) The fluorescence spectra of **TPEPy-SS-C14** (10 μmol/L) in water/dimethyl sulfoxide (DMSO) mixtures with different H_2O fractions. (c) The plot of the relative emission intensity (I/I_0) of **TPEPy-SS-C14** *versus* the H_2O fractions in H_2O/DMSO mixtures. Inset: Tyndall experiment of **TPEPy-SS-C14** (10 μmol/L) in the DMSO solution and in H_2O/DMSO mixtures with 90% H_2O fractions under 365 nm UV irradiation. (d) Size distribution of **TPEPy-SS-C14** (10 μmol/L). Inset: SEM image of **TPEPy-SS-C14** (10 μmol/L). The fluorescence emission spectrum of **TPEPy-SS-C14** (10 μmol/L) after adding different amounts of ATP (e) and H_2S (f) in HEPES (10 mmol/L, pH 7.4) buffer solution. (g) Photographs of **TPEPy-SS-C14** (10 μmol/L) for ATP (0.17 mmol/L) and H_2S (55 mmol/L) under 365 nm UV irradiation. (h) The fluorescence spectra of **TPEPy-SS-C14** (10 μmol/L) after addition of ATP (0.17 mmol/L) or H_2S (55 mmol/L). The excitation wavelength is 420 nm.

rhodamine and recognize H_2S by the reduction of -N_3 on 1,8-naphthalimide. These probes have complex synthesis process and single recognition mechanism, but here we design and synthesize a novel AIE bifunctional probe **TPEPy-SS-C14**, which can simultaneously detect ATP and H_2S based on the aggregation/disaggregation mechanism. **TPEPy-SS-C14** can detect ATP with a fluorescence enhancement response due to complexation enhanced aggregation. And H_2S can quench the fluorescence due to the disaggregation of the cleavable disulfide bond. In addition, the probe locates mitochondria, and can detect ATP and hydrogen sulfide levels in living cells.

The specific guest induced aggregation-disaggregation mechanism of **TPEPy-SS-C14** to detect ATP and H_2S are shown in Scheme 1. Upon the addition of ATP, strong intermolecular interactions will occur between pyridinium and amide donors of **TPEPy-SS-C14** and the negative phosphate groups of ATP. This proposed binding model can be confirmed by ^1H NMR titration of **TPEPy-SS-C14** with ATP in DMSO-d_6/D_2O (8:2, v/v) solution, therein a large chemical shift was observed in the pyridinium and amide protons (Fig. S10 in Supporting information). After binding with ATP, the nano-aggregation of **TPEPy-SS-C14** became larger, with the DLS data changing from 180 nm to 360 nm in aqueous solution, and the transmission electron microscope (TEM) increasing up to 340 nm in solid state (Fig. S11 in Supporting information). Thus, the complexation of ATP can enhance the aggregation of **TPEPy-SS-C14**, which makes the fluorescence a turn-on response. We also investigated the reaction mechanism of **TPEPy-SS-C14** toward H_2S by high-resolution mass spectrum. In Fig. S12 (Supporting information), after treated with H_2S, **TPEPy-SS-C14** is cleaved into **TPEPy-SSH**, **C14-SSH** and **C14-SS-C14** species, indication that the addition of H_2S leads to disaggregation.

Next, we studied the sensing performance of **TPEPy-SS-C14** in the simultaneous detection of ATP and H_2S in HEPES buffer. **TPEPy-SS-C14** still can detect H_2S effectively in the presence of ATP, but can not recognize ATP with the coexistence in H_2S (Figs. 1g and h). We further tested the concentration dependent change of H_2S added with ATP. From Fig. S13 (Supporting information), we can see that the fluorescence of **TPEPy-SS-C14** at 630 nm first increase upon addition of ATP for complexation. The fluorescence intensity gradually decreases when further addition of H_2S, with the quenching ratio as high as 94%. Interesting, the calculated LOD of **TPEPy-SS-C14**/ATP toward H_2S is 1.57×10^{-7} mol/L, which is lower than that of **TPEPy-SS-C14** (5.0×10^{-7} mol/L). This result is reasonable because the H_2S trigged disulfide bond cleavage can happen in both **TPEPy-SS-C14** and **TPEPy-SS-C14**/ATP nano-aggregation. The addition of ATP will not affect the quenching effect of hydrogen sulfide on **TPEPy-SS-C14** probe.

To further study the specificity of **TPEPy-SS-C14** for ATP and H_2S, the responses of the probe to other interfering species, including metal cations, various anions and amino acids were also studied (Fig. 2a). As shown in Fig. 2b and Fig. S14 (Supporting information), a few other phosphate anions, for example, adenosine diphosphate (ADP), adenosine monophosphate (AMP), pyrophosphate (PPi) and inorganic phosphate (Pi), can also slightly enhance the fluorescence. A weak response to ADP, PPi, Pi and AMP, with a partial enhance of the emission spectra of **TPEPy-SS-C14** was recorded in Figs. S15 and S16 (Supporting information). However, this interference can be ignored because **TPEPy-SS-C14** exhibits far better binding affinity of ATP than these similar structured polyphostates. The detection limits and binding constants of **TPEPy-SS-C14** to these anions were also shown in Table S2 (Supporting information). Particularly, the K_{ATP}/K_{ADP} ratio is about 230.

On the other hand, we find the addition of some thiols-containing amide acid, including glutathione (GSH), cysteine (Cys) and homocysteine (Hcy), can also leads to a little decrease of the fluorescence. However, the quench ratio by the thiols is much

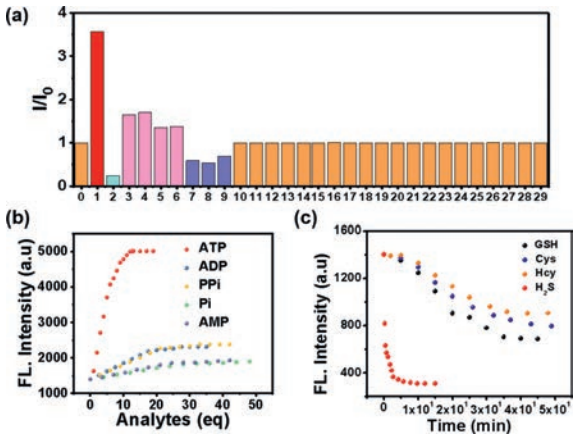

Fig. 2. (a) Relative fluorescence histogram chart of **TPEPy-SS-C14** (10 μmol/L) at 630 nm upon the addition of 0.55 mmol/L various analytes, 0-free, 1-ATP, 2-H_2S, 3-ADP, 4-PPi, 5-AMP, 6-Pi, 7-GSH, 8-Cys, 9-Hcy, 10-CH_3COO^-, 11-NO_3^-, 12-Cl^-, 13-Br^-, 14-HSO_4^-, 15-SO_3^{2-}, 16-Glu, 17-Arg, 18-His, 19-Met, 20-Thr, 21-Ser, 22-K^+, 23-Na^+, 24-Ca^{2+}, 25-Mg^{2+}, 26-Fe^{2+}, 27-Fe^{3+}, 28-Zn^{2+}, 29-Al^{3+}. (b) Fluorescence intensities of **TPEPy-SS-C14** at 630 nm *versus* the number of equivalents of several phosphate anions. (c) Time-dependent fluorescence intensity at 630 nm of **TPEPy-SS-C14** (10 μmol/L) upon addition of 55 equivalents of biothiols in HEPES buffer solution (pH 7.4).

lower than that of H_2S, indicating that **TPEPy-SS-C14** can discriminate H_2S from thiols and other analytes. The difference fluorescence response of **TPEPy-SS-C14** toward H_2S and thiols may be attributed their different reaction mechanism. For H_2S, which mainly exists as HS^- in physiological conditions, can effectively cleave the disulfide bond to release the fluorescent active species **TPEPy-SSH** [8–12]. However, the thiols reaction may give both the cleavage and the disulfide exchange products. We also studied the reaction mechanism of GSH with the probe (Fig. S17 in Supporting information), which captures not only the cleavage product **TPEPy-SH**, but also the disulfide exchange species **TPEPy-SG**. Regarding that **TPEPy-SG** is also amphiphily for bearing the hydrophilic glutathione group, it may exhibit self-assembly property with high emission. Therefore, the fluorescence is only slightly reduced after adding GSH and other thiols [26]. Furthermore, H_2S shows stronger nucleophilicity than bio-thiols. We compared the time kinetics of H_2S and other thiols with **TPEPy-SS-C14** (Fig. 2c), and found that the fluorescence of hydrogen sulfide added decreased rapidly in a few seconds, and basically reached equilibrium in 5 min, while other thiols took nearly 50 min. So probe **TPEPy-SS-C14** reacting with H_2S is dominant under the complexed physiological conditions.

For really application, a good multifunctional probe should also behaves an excellent selectively in many competitive ions. Thus, the competitive experiments of **TPEPy-SS-C14** toward ATP/H_2S under the coexistence of many interference species were carried out (Fig. S18 in Supporting information). It was revealed that **TPEPy-SS-C14** still displays a excellent fluorescence enhancement ability toward ATP in the presence of these analytes, except H_2S. However, it can recognize H_2S in the presence of the following 27 analytes, containing biothiols GSH, Cys and Hcy (Fig. S19 in Supporting information). In addition, the influences of pH experiments reveals that this probe can work in wide pH range of 6–10, indicating the physiological applicability of the **TPEPy-SS-C14** probe (Fig. S20 in Supporting information).

Based on the good selective competition and anti-interference ability of the probe *in vitro*, **TPEPy-SS-C14** was used to recognize ATP and H_2S in living cells. Firstly, the toxicity of **TPEPy-SS-C14** on SMMC cells was conducted by standard MTT assay. As shown in Fig. S21 (Supporting information), **TPEPy-SS-C14** possessed a low

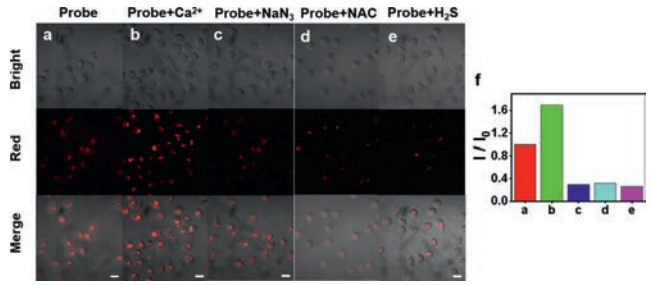

Fig. 3. Confocal laser scanning microscopy (CLSM) images of SMMC cells that were incubated with **TPEPy-SS-C14** (10 μmol/L) for 45 min (a). Cells were pretreated with Ca^{2+} (1.5 mmol/L; 1 h) (b), NaN_3 (1.5 mmol/L; 1 h) (c), *N*-acetyl-L-cysteine (NAC) (1 mmol/L; 1 h) (d), Na_2S (0.6 mmol/L; 1 h) (e), followed incubation with **TPEPy-SS-C14** (10 μmol/L) for another 45 min, respectively. (f) Relative fluorescence intensity of a, b, c, d and e. Scale bar: 20 μm. $\lambda_{ex} = 488$ nm, $\lambda_{em} = 570–700$ nm.

cytotoxicity at the test concentration and is appropriate for intracellular imaging. The subcellular location of **TPEPy-SS-C14** was investigated by co localization experiment with Mito tracker green. **TPEPy-SS-C14** overlaps well with Mito tracker green dye, with an overlap rate of 0.91 (Fig. S22 in Supporting information). These results show that **TPEPy-SS-C14** has a good localization effect on mitochondria and provides the imaging ability of ATP and hydrogen sulfide in mitochondria.

In order to investigate the ability of **TPEPy-SS-C14** to recognize ATP in cells, we divided the cells into three groups: control group (row a), calcium ion treated (row b) and sodium azide treated (row c) (Fig. 3). Ca^{2+} increases ATP concentration by activating mitochondrial dehydrogenase and the fluorescence intensity of corresponding cell imaging is 120% of that of the control group. On the contrary, sodium azide will inhibit enzyme activity, leading to the decrease of ATP concentration and the fluorescence intensity of corresponding cell imaging is only 29% of that of the control group. This indicates that the probe can successfully detect the level of ATP in cells.

Then, we evaluated the imaging ability of **TPEPy-SS-C14** for endogenous and exogenous H_2S. In Fig. 3, after incubating the cells pretreated with NAC (1 mmol/L) with 10 μmol/L probes for 1 h, the red fluorescence decreased significantly (row d), indicating that NAC induced the production of endogenous hydrogen sulfide concentration, and leaded to cleavage **TPEPy-SS-C14** in living cells. Similarly, the fluorescence of cells treated with exogenous H_2S was also reduced obviously as expected (row e). These results demonstrate that **TPEPy-SS-C14** can effectively evaluate the level of endogenous and exogenous H_2S in cells. Probe **TPEPy-SS-C14** can be applied as a tool to explore the level of ATP and hydrogen sulfide in living cell mitochondria.

To sum up, we constructed a dual site AIE fluorescence probe **TPEPy-SS-C14** and proposed a new strategy of assembly/disassembly for simultaneous recognition of ATP and H_2S. As a proof of concept, the assembly/disassembly mechanism was applied to modulate the fluorescence of the amphiphilic AIEgen. After interaction ATP or H_2S with probe, the aggregation state of the probe in the aqueous solution changes, showing that the fluorescence increases or decreases. It is worth mentioning that **TPEPy-SS-C14** has good sensitivity and selectivity to ATP and hydrogen sulfide in SMMC cells under physiological conditions. This system has superiority over previously reported work, such as easier synthesis, lower detection limit, shorter detection time and simple operation. The sensor possesses the potential to become a effective tool to research the relationship between ATP and H_2S in mitochondria of living cells.

Declaration of competing interest

The authors declare that they have no known competing financial interests or personal relationships that could have appeared to influence the work reported in this paper.

Acknowledgments

This work was supported by the National Nature Science Foundation of China (No. 22061028) and Jiangxi Provincial Natural Science Foundation (No. 20224ACB203012).

Supplementary materials

Supplementary material associated with this article can be found, in the online version, at doi:10.1016/j.cclet.2023.108925.

References

[1] C.F. Higgin, I.D. Hiles, G.P.C. Salmond, et al., Nature 323 (1986) 448–450.
[2] P.B. Dennis, A. Jaeschke, M. Saitoh, et al., Science 294 (2001) 1102–1105.
[3] K.T. Bush, S.H. Keller, S.K. Nigam, J. Clin. Invest. 106 (2000) 621–626.
[4] D.H. Matthew, D.P. Michael, Chem Soc. Rev. 45 (2016) 6108–6117.
[5] D. Hanahan, A.W. Robert, Cell 144 (2011) 646–674.
[6] D. Giuliani, A. Ottani, D. Zaffe, et al., Neurobiol. Learn. Mem. 104 (2013) 82–91.
[7] B.H. Huang, B. Liang, R.S. Zhang, D.M. Xing, Coord. Chem. Rev. 452 (2022) 214302.
[8] Y. Zhou, Z.C. Xu, Y.Y. Ju, Chem. Soc. Rev. 40 (2011) 2222–2235.
[9] J.B. Stephen, A.J. Katrina, ChemPlusChem 86 (2021) 59–70.
[10] X. Zhou, X. Wang, L. Shang, Chin. Chem. Lett. 34 (2023) 108093.
[11] H. Duan, F. Cao, M. Zhang, M. Gao, L. Cao, Chin. Chem. Lett. 33 (2022) 2459–2463.
[12] L. Jiang, T. Chen, E. Song, Chem. Eng. J. 427 (2022) 131563.
[13] M.W. Yang, J.L. Fan, J.J. Du, X.J. Peng, Chem. Sci. 11 (2020) 5127–5141.
[14] Z. Fang, Z. Su, W. Qin, et al., Chin. Chem. Lett. 31 (2020) 2903–2908.
[15] L.L. Wu, J.G. Huang, K.Y. Pu, T.D. James, Nat. Rev. Chem. 5 (2021) 406–421.
[16] J.Y. Guo, B. Fang, H. Bai, et al., Trends Anal. Chem. 155 (2022) 116697.
[17] J.L. Kolanowski, F. Liu, J. Elizabeth, Chem. Soc. Rev. 47 (2018) 195–208.
[18] X. Chai, Z.T. Fan, M.M. Yu, J. Zhao, L.L. Li, Nano Lett. 21 (2021) 10047–10053.
[19] W.J. Zhang, Y.X. Lu, F.J. Huo, Y.B. Zhang, C.X. Yin, Dyes Pigm. 204 (2022) 110442.
[20] X.P. Yang, P.Y. Xie, J.F. Liu, et al., Chem. Eng. J. 442 (2022) 136–141.
[21] P.P. Sun, H.C. Chen, S.Y. Lu, et al., Anal. Chem. 94 (2022) 11573–11581.
[22] Y. Fang, W. Shi, Y.M. Hu, X.H. Li, H.M. Ma, Chem. Commun. 54 (2018) 5454–5457.
[23] Z. Wu, M.M. Liu, Z.C. Liu, Y. Tian, J. Am. Chem. Soc. 142 (2020) 7532–7541.
[24] L.L. Wu, J.H. Liu, X. Tian, et al., J. Am. Chem. Soc. 144 (2022) 174–183.
[25] H. Tao, L. He, G.J.S. Cheng, Q.Y. Cao, Dyes Pigm. 166 (2019) 233–238.
[26] A. Shamirian, H.S. Afsari, D. Wu, L.W. Miller, P.T. Snee, Anal. Chem. 88 (2016) 6050–6056.